Preliminary draft 17:58 28 March 2019

28 March 2019
niloufar.alipour.tehrani@cern.ch

Simulation studies for a drift chamber at the FCC-ee experiment

Niloufar Alipour Tehrani
CERN, CH-1211 Geneva, Switzerland

Keywords:

Summary

The physics aims at the electron-positron option for the Future Circular Collider (FCC-ee) [6], impose high precision requirements on the vertex and tracking detectors. The detector has also to match the experimental conditions such as the collisions rate and the presence of beam-induced backgrounds. A light weight tracking detector is under investigation for the IDEA (International Detector for Electron-Positron Accelerator) detector concept and consists of a drift chamber. Simulation studies of the drift chamber using the FCCSW (FCC software) are presented. Full simulations are used to study the effect of beam-induced backgrounds on this detector.

Contents

1 Introduction

The FCC-ee high-luminosity circular electron-positron collider, with center-of-mass energies $\sqrt{s}$ from 91.2 GeV to 365 GeV, allows for high-precision measurements of the properties of the Z, the W, the top quark and the Higgs boson. As a predecessor of a new 100 TeV proton-proton collider, the FCC-ee collider is foreseen to be placed in a 100 km tunnel in Geneva area as shown in Fig. 1.

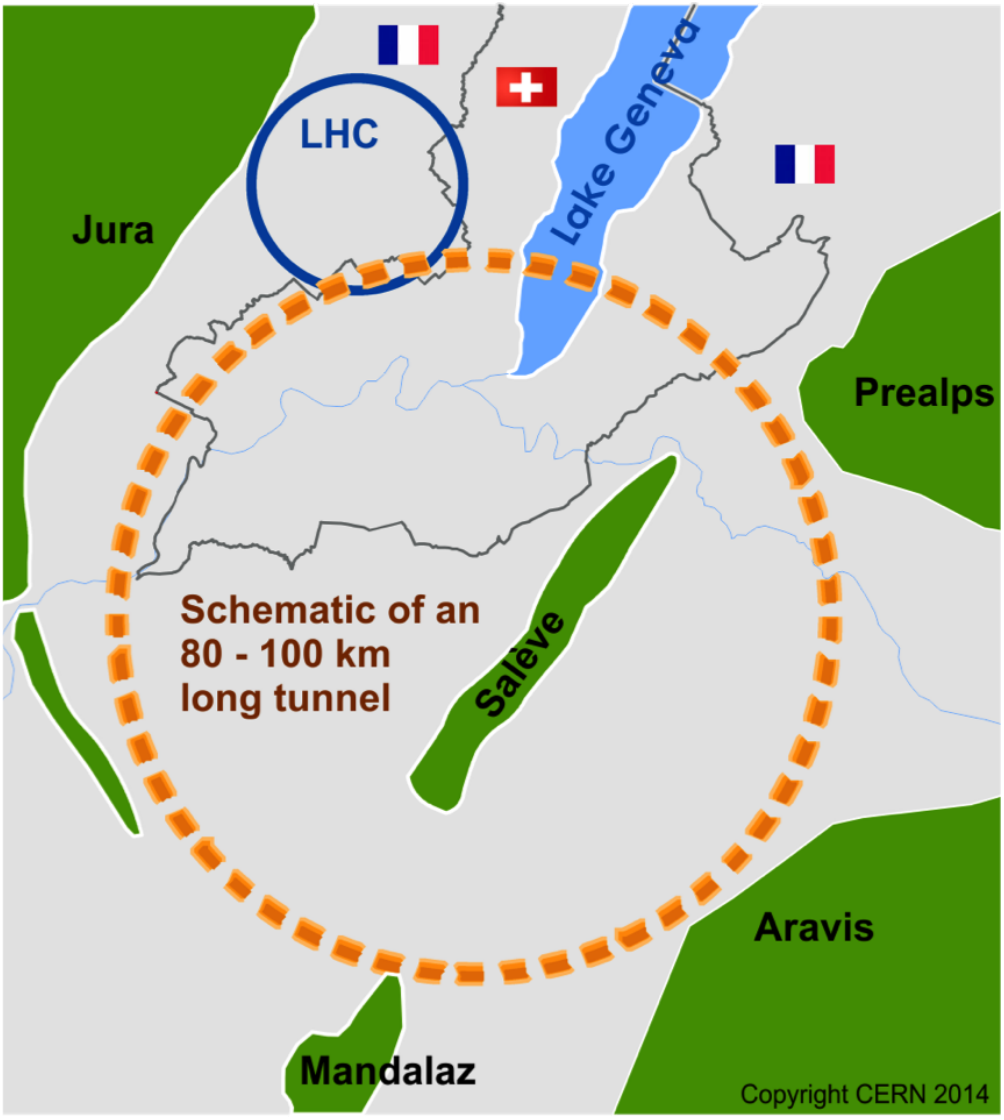

Figure 1: A possible realization of the FCC experiment near the Geneva region.

The IDEA detector, one of the two detector concepts under development for FCC-ee, has demanding requirements to match the experimental conditions. Its main components consist of: an ultra-light silicon-based vertex detector, an ultra-light drift chamber for track reconstruction and particle identification, a dual-readout calorimeter, a 2 T axial magnetic field and an instrumented return yoke as illustrated in Fig. 2. The drift chamber is being investigated using GEANT4-based simulations. Its performance and the effect of beam-

induced backgrounds are presented here-below.

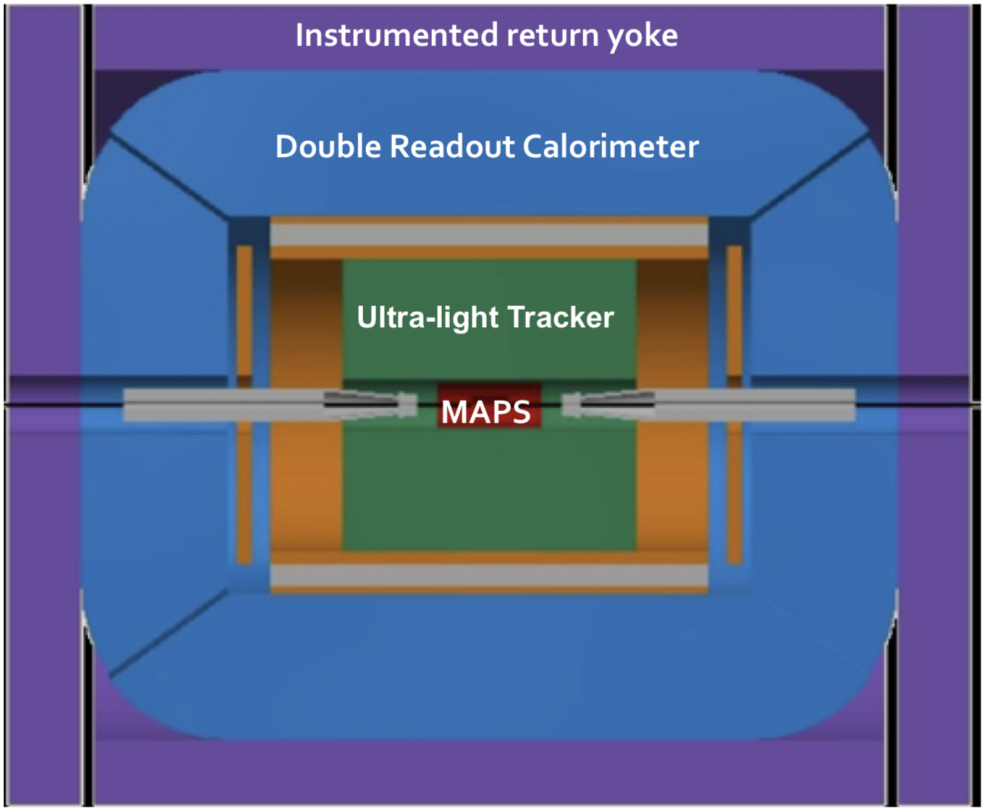

Figure 2: Schematic layout of the IDEA detector with the sub-detectors illustrated in different colors: vertex detector (red), drift chamber (green), pre-shower (orange), magnet (gray), calorimeter (blue), magnet yoke and muon system (violet).

2 Drift chamber

The drift chamber (DCH) is optimized to provide excellent tracking, high precision momentum measurement and excellent particle identification using cluster counting technique with an extremely low material content.

The drift chamber for IDEA is based on the drift chamber for the KLOE experiment [7] as well as a more recent version of it developed for the MEG2 experiment [4].

The drift chamber consists of a unique-volume with high granularity. It is foreseen to use a gas composed of 90 % of Helium and 10 % of isobutane (C_4H_{10}). It is composed of 112 co-axial layer with wires having an average stereo angle of 0.1 radians allowing for a longitudinal resolution of 1 mm. The square cell size varies between 12.0 mm and 14.5 mm. The parameters of the drift chamber for the IDEA detector are summarized in Table 1. The description of the simulation chain for the drift chamber using the FCCSW is described here-below.

Table 1: Parameters of the drift chamber for the IDEA detector

Length	4 m
Inner radius	0.345 m
Outer radius	2 m
Number of sensitive wires	56'448
Transverse resolution	0.1 mm
Longitudinal resolution	1 mm
Material content in radial direction	1.6%
Material content in the forward direction	5.0 %

3 Simulation with the FCC Software

The FCC Software (FCCSW) [2] is a common software for all FCC experiments. It is based on the Gaudi software framework [5] for parallel data processing, GEANT4 simulation toolkit [3] and the DD4hep detector description toolkit for high energy physics [8]. The FCCSW simulation pipeline is summarized in Fig. 3 and described here-below.

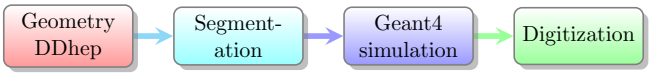

Figure 3: The FCCSW simulation chain.

3.1 Geometry description with DD4hep

First, the geometry of the detector is described using the DD4hep simulation framework. The current implementation of the detectors in the interaction region for the IDEA detector is shown in Fig. 4. The interaction region consists of a beam pipe, a shielding solenoid, a luminosity calorimeter, a vertex detector and a drift chamber. The geometry of the drift chamber is defined as layers of gas. In order to increase the simulation speed, the individual wires are not physically placed in the simulation software and the segmentation takes them into account.

3.2 Segmentation

The segmentation of the sensitive gas detector contains the information on the positions of the wires in the detector. The segmentation for the first layer of the drift chamber is shown in Fig. 5. This reduces the running time by avoiding to place each wire volume individually.

The total number of wires as a function of the polar angle θ is illustrated in Fig. 6. In the barrel region, a high coverage is obtained by $\sim$ 112 wires in average. In the forward region, silicon disks are foreseen to improve the track angle coverage.

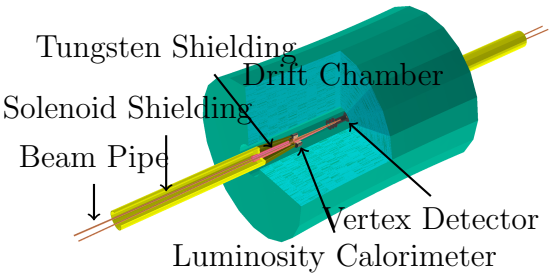

Figure 4: The detectors at the interaction region for the FCC-ee IDEA concept as implemented in FCCSW.

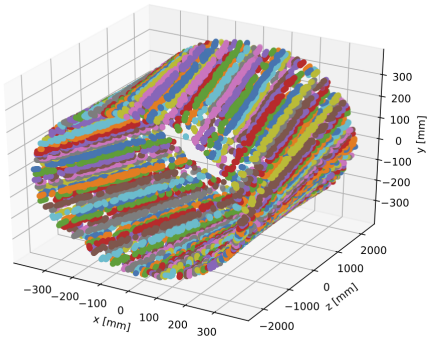

Figure 5: The segmentation of the first layer of the drift chamber.

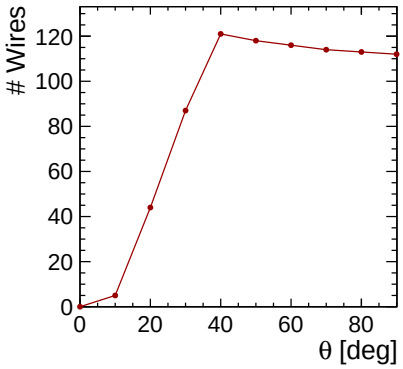

Figure 6: Total number of wires as a function of the polar angle θ (calculated using infinite momentum tracks from the origin).

3.3 Geant4 simulation and digitization

GEANT4 simulates the passage of particles through matter. For the drift chamber simulation, a step size of 2 mm is chosen in order to step trough the gas volume and calculate the energy deposited. The ionization charge is then drifted to the nearest wire. This allows for calculating the drift time and therefore the signal in the wires. Once the contribution from each GEANT4 step is calculated, the digitization step regroups the energy deposited with a drift time smaller than the maximum drift time in the cell.

4 Impact of beam-induced backgrounds

Three main sources of beam-induced backgrounds at the FCC-ee experiment are: incoherent e^+e^- pairs, $\gamma\gamma \rightarrow$ hadrons and the synchrotron radiation. Each background source is studied below.

The incoherent e^+e^- pairs are generated from the strong electromagnetic force from the electron and positron bunches in the field of the opposite beam. This leads to the production of Beamstrahlung photons. The interactions of Beamstrahlung photons generate incoherent lepton pairs at low polar angles and mostly contained in the forward direction as shown in Fig. 7. The GUINEA-PIG [10] event generator has been used to generate the incoherent e^+e^- background particles at a $\sqrt{s}$ of 91.2 GeV and 365 GeV [11] and their impact on the drift chamber is simulated using the FCCSW. The occupancy of the drift chamber due to incoherent e^+e^- pairs as a function of the detector radius is shown in Fig. 8. In fact, the produced incoherent pairs have a low polar angle and only few of them reach the drift chamber. Most of the hits observed are due to the scattering of the e^+e^- pairs by interacting with the elements in the interaction region.

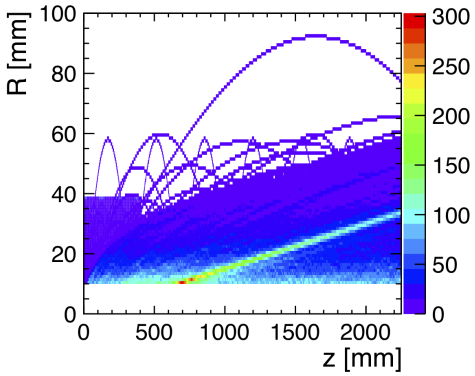

Figure 7: The trajectory of the e^+e^- pairs in a 2 T magnetic field.

The $\gamma\gamma \rightarrow$ hadrons background is expected to have a very low impact on the drift chamber. The synchrotron radiation, dictates the design of the interaction region. It defines the beampipe radius and the design of the shielding (in Tungsten). Table 2 summarizes the occupancy in the drift chamber due to different sources of beam-induced backgrounds. The overall occupancy due to all backgrounds is as expected, with e^+e^- pair background having the highest impact. Based on previous experience with the MEG2 experiment, it can be deduced that the background does not pose problem for the reconstruction of the tracks using the drift chamber.

5 Tracking

The drift chamber, with 112 layers of wires, provides high number of measurements which can be exploited for the track reconstruction.

One of the methods we are investigated is the Hough transform as described below.

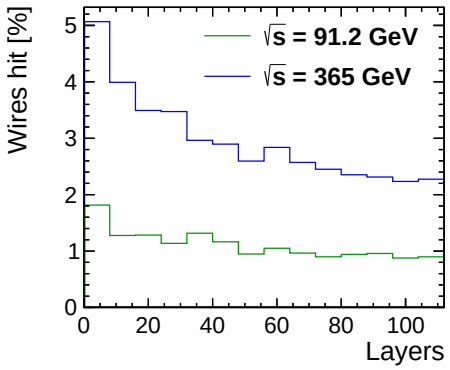

Figure 8: The percentage of wires hit due to e^+e^- pair background as a function of the layer radius averaged over 100 bunch crossings. For the Z stage ($\sqrt{s} = 91.2$ GeV), the readout latency is also taken into account by summing up the background over 4 bunch crossings.

Table 2: Average occupancy in the drift chamber due to beam-induced backgrounds.

Background	Average occupancy	
	$\sqrt{s} = 91.2$ GeV	$\sqrt{s} = 365$ GeV
e^+e^- pair background	1.1%	2.9%
$\gamma\gamma \to$ hadrons	0.001%	0.035%
Synchrotron radiation	negligible	0.2%

5.1 The Hough Transform

Initially invented for bubble chamber photographs [1], the Hough Transform is a feature extraction technique used in several fields such as image analysis, computer vision and digital image procession. It allows for the identification of lines as well as other shapes such as circles or ellipses.

5.1.1 Principle

The simplest case of Hough transform is detecting straight lines. In the parameter space, lines are represented as a point (b, m) with Eq. (1).

$$y = m \cdot x + b \tag{1}$$

With the presentation (b, m) in the parameter space, vertical lines pose problems for the unbounded slope parameter m. The Hesse normal form as described in Eq. (2) can be used as a solution to get around vertical lines, where r is the shortest distance from the origin to the line and θ is the angle between the x axis and the line connecting the origin with the closest point as illustrated in Fig. 9. The (r, θ) plane is referred to as the Hough Space.

$$r = x \cdot \cos(\theta) + y \cdot \sin(\theta) \tag{2}$$

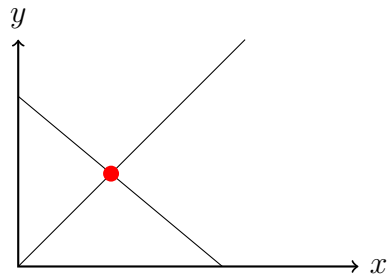

Figure 9: TODO: A line is representate as a point (b, m) in the parameter space according to Eq. (1).

Section 5.1.1 shows the Hough transformation applied to every point on a line. In the Hough space, all the points on the line are represented by a local maximum since they all have the same (r, θ) value.

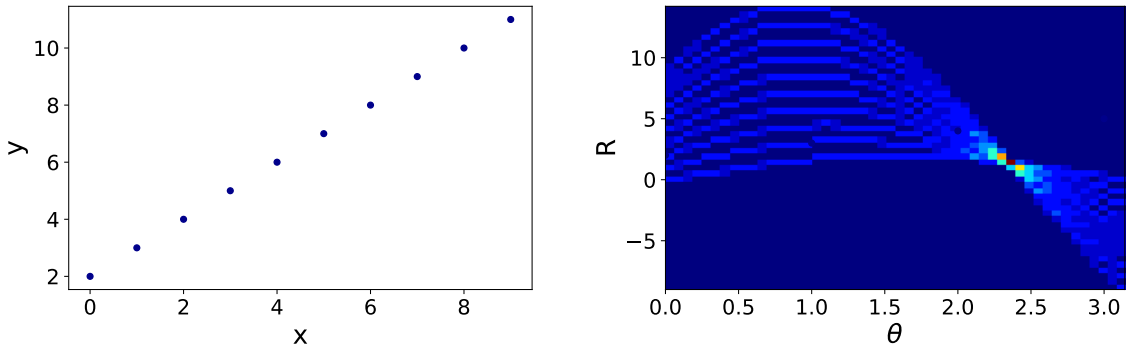

(a) Parameter space

(b) Hough space

Figure 10: A line as represented in the parameter and the Hough space.

5.1.2 Identification of circles

The track of a charged particle in a magnetic field follows a helicoidal trajectory. In the xy-plane, the hits follow a circular trajectory as described with Eq. (3) where (a, b) represent the center of the circle and R the radius of the circle.

$$(x - a)^2 + (y - b)^2 = R^2 \tag{3}$$

The Hough transformation gets better results when applied to lines. For this reason, first the conformal mapping [9] is first applied to map circular hits into lines using Eq. (4).

$$u = \frac{x}{x^2 + y^2}, \quad v = \frac{y}{x^2 + y^2} \tag{4}$$

The conformal mapping maps a circle to a line if and only if the circle passes from the origin or following the condition as described in Eq. (5) and the straight lines are described by Eq. (6).

$$a^2 + b^2 = R^2 \tag{5}$$

$$v = \frac{1}{2b} - u\frac{a}{b} \tag{6}$$

If the condition in Eq. (5) is not satisfied, some correction terms are needed for the transformation in Eq. (4) to transform circles into lines.

The Hough transformation is then applied to the straight lines using Eq. (7).

$$\rho = u \cdot cos(\phi) + v \cdot sin(\phi) \tag{7}$$

The radius of the circle R is connected the ρ parameter of the Hough transformation by Eq. (8).

$$R = \frac{1}{2 \cdot \rho} \tag{8}$$

Finally, the center of the circle is extracted from the Hough transformation using Eq. (9).

$$a = \frac{cos(\phi)}{2 \cdot \rho}, \quad b = \frac{sin(\phi)}{2 \cdot \rho} \tag{9}$$

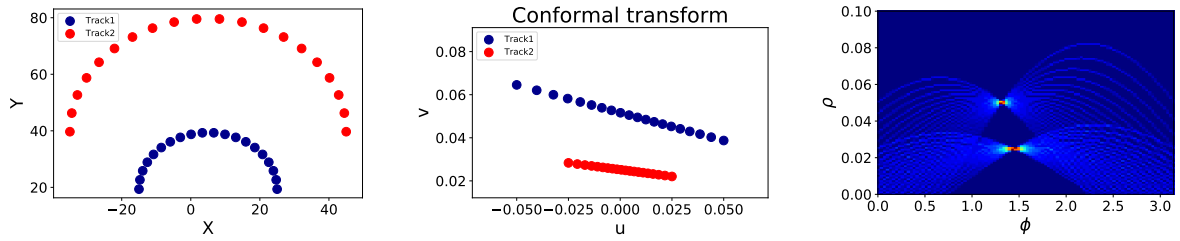

(a) (b) (c)

Figure 11: Circles (a) as represented after a conformal mapping (b) and after the Hough transformation (c).

5.1.3 Hough transform for helix

5.2 Results for particle gun

5.3 Hough transformation and the simulation of jets

For a center-of-mass energy of $\sqrt{s} = 91$ GeV, the simulation of the jets by the decay $Z \rightarrow d\bar{d}$

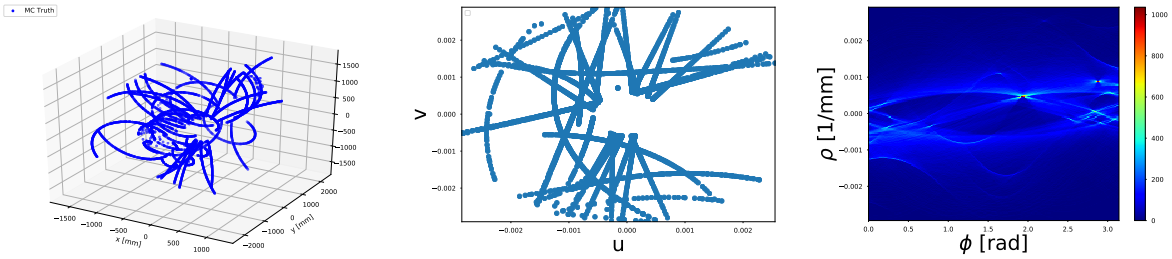

(a) (b) (c)

Figure 12: $Z \to d\bar{d}$

References

[1] Hough transform.

[2] The Future Circular Collider Software Framework.

[3] S. Agostinelli et al. GEANT4: A Simulation toolkit. *Nucl. Instrum. Meth.*, A506:250–303, 2003.

[4] A. M. Baldini et al. The design of the MEG II experiment. *Eur. Phys. J.*, C78(5):380, 2018.

[5] G. Barrand et al. GAUDI - A software architecture and framework for building HEP data processing applications. *Comput. Phys. Commun.*, 140:45–55, 2001.

[6] M. Bicer et al. First Look at the Physics Case of TLEP. *JHEP*, 01:164, 2014.

[7] Erika De Lucia. Status of the KLOE-2 Inner Tracker. *EPJ Web Conf.*, 166:00003, 2018.

[8] M. Frank, F. Gaede, and P. Mato. DD4hep: A Detector Description Toolkit for High Energy Physics Experiments. *J. Phys.: Conf. Ser.*, 513(AIDA-CONF-2014-004):022010, Oct 2013.

[9] M. Hansroul, H. Jeremie, and D. Savard. FAST CIRCLE FIT WITH THE CONFORMAL MAPPING METHOD. *Submitted to: Nucl. Instrum. Methods*, 1988.

[10] Daniel Schulte. Beam-Beam Simulations with GUINEA-PIG. Mar 1999.

[11] Georgios Voutsinas, Nicola Bacchetta, Manuela Boscolo, Patrick Janot, Anna Kolano, Emmanuelle Perez, Michael Sullivan, and Niloufar Tehrani. Luminosity- and Beam-Induced Backgrounds for the FCC-ee Interaction Region Design. In *Proceedings, 8th International Particle Accelerator Conference (IPAC 2017): Copenhagen, Denmark, May 14-19, 2017*, page WEPIK004, 2017.